International Journal of Innovative
Computing, Information and Control
Volume **14**, Number **2**, April **2018**

ICIC International ©2018 ISSN 1349-4198
pp. **469–489**

ANALYSIS OF BUSINESS LOSS AND SYSTEM RISK CAUSED BY NONSTANDARD AND EXCESSIVE QUALITY

Kenji Shirai[1] and Yoshinori Amano[2]

[1]Faculty of Information Culture
Niigata University of International and Information Studies
3-1-1, Mizukino, Nishi-ku, Niigata 950-2292, Japan
shirai@nuis.ac.jp

[2]Kyohnan Elecs Co., LTD.
8-48-2, Fukakusanishiura-cho, Fushimi-ku, Kyoto 612-0029, Japan
y_amano@kyohnan-elecs.co.jp

Received August 2017; revised December 2017

Abstract. *The loss function by Professor G. Taguchi is defined by the quality as "losses to be given to society after shipment, but excluding losses due to the function itself". Furthermore, he proposed an evaluation with a loss function that approximates that the loss is proportional to the square of the deviation from the target, and it was economically reasonable that the quality control using the standard deviation and the least squares method are appropriate. The probability distribution of the quality of main manufacturing parts (hybrid integrated chips) used in products is assumed to be a normal distribution. The distribution function gives the probability density function of the quality measurements for the individual products, and we here introduce a major loss function in quality engineering. Generally, the shipping-side standard and the receiving-side standard differ; therefore, the underquality and overquality are analyzed. The loss cost significantly fluctuates because of product quality problems, process lead time, and so forth, thereby affecting the profit risk. These system risks can be mathematically analyzed. We report calculation results for process risk probability based on actual data.*

Keywords: Loss function, Normal distribution, Underquality, Overquality, Process lead time

1. **Introduction.** Professor G. Taguchi established the Quality Engineering Forum in 1993 (now the Quality Engineering Society) under the premise of advancing quality engineering as an academic pursuit. In the Taguchi method, the magnitude of the difference from the desired state is determined such that the definition of error is "measured value – true value" [1]. The proper assessment of errors is essential for cost reduction and for ensuring reliability. A potential for loss exists near the design value limit. Dr. Taguchi said that "discussion of comprehensive judgment of technology is necessary". However, many companies have overlooked the role and responsibility of technicians as a consequence of partial short-term work.

We describe why the loss function has a negative indicator of loss. For example, users, who bought a product that can only exercise the marginal function of the standard value, will mostly "feel dissatisfied". In other words, it is the best way to express the quality of the product as a negative indication of "dissatisfaction degree". Strategic technicians believe that the "overall optimization" of the system for change of goods should be considered and linked to minimization of the social loss of the sum of quality and cost. That is, the purpose of works, efficiently improving manufacturing methods, and expanding the freedom of individuals make extra time available for workers to engage with new work and hobbies. With respect to Dr. Taguchi's loss function, the definition of quality includes various factors. He stated "whole characteristics of features or services that meet their needs or abilities". A tolerance can be set by introducing a loss function, which is an indispensable item for cost reduction and reliability assurance. A potential for loss exists near the production quality limit of the design value. In addition, the loss function is proportional to the volatility at the set value.

The traditional approach to avoiding bottlenecks in production processes is to use the theory of constraints [2], and we have reported that the synchronized method is superior for shortening throughput in production processes. This method requires synchronization between processes [3, 4, 5].

In our previous study [6, 7], we constructed a state in which the production density of each process corresponded to the physical propagation of heat [8]. Using this approach, we showed that a diffusion equation dominates the production process. In other words, when minimizing the potential of the production field (stochastic field), the equation, which is defined by the production density function $S_i(x,t)$ and boundary conditions, is described by the use of diffusion equation with advection to move in transportation speed ρ. The boundary conditions describe a closed system in the production field. The adiabatic state in thermodynamics represents the same state [6].

With respect to the production flow system, generally, low volumes of a wide variety of products are produced through several stages in the production process. This method is good for producing specific control equipment such as semiconductor manufacturing equipment in our experience. We have reported many research findings in this area. The production flow process has nonlinear characteristics [9]. Moreover, we have made it clear that the manufacture of products proceeds in multiple stages from the beginning of production. Such volatility is encountered in every stage of manufacturing, and delays in the production line propagate this volatility to the successive steps. A delay in the production process is equivalent to a "fluctuation" in physical phenomena [10].

On the other hand, there are several reports on evaluation and risk management of production processes utilizing mathematical finance. With respect to financial analysis, a rate of return and volatility at the time of long term investment was researched to compare a rate of return and volatility of short term investment [11, 12]. In this research, Monte Carlo method was utilized in order to simulate a rate of return. Further, there is a report saying that, as a result of investigation of long-term return on investment and its dispersion characteristics, geometric Brownian motion models describing a price of risk assets differ substantially from actual phenomenon [13]. To achieve the production system goals, we propose the use of a mathematical model that focuses on the selection process and adaptation mechanism of the production lead time [6, 14]. We model the throughput time of the production demand/production system in the production stage by using a stochastic differential equation of the log-normal type, which is derived from its dynamic behavior. Using this model and risk-neutral integral, we define and compute the evaluation equation for the compatibility condition of the production lead time. Furthermore, we apply the synchronization process and show that the throughput of the production process is reduced [6, 15].

In this paper, first, we analyze overquality and underquality existing in the quality distribution (normal distribution). Next, based on the analysis result, the simulation results of expected loss function for several parameter values are presented. We show real variations of cases where volatility greatly affects the production lead time. Finally, we analyze the process lead time risk and show the simulation results. We present the results that the average number of production is high and the production process with low volatility shows low risk.

A normal distribution was assumed as a probability density function of measured values for individual products. In the statistical quality control method, quality managers generally adopt a normal distribution to deal with volatilities. Also, in order to grasp the quality quantitatively, it is absolutely necessary to introduce a normal distribution as a probability distribution. Products that are completed through the production processes necessarily involve volatilities. To statistically grasp this volatility, a probability distribution is required, and among them, a normal distribution is often used. By dealing with under- and excessive-quality, customer satisfaction will be improved. We also introduce the loss function for deviation from the design value m. By using the probability distribution and the loss function of the individual products (hybrid integrated chips), we obtain the occurrence probability of defective products out of specification and of products with within-standard excessive quality. The goal is for quality problems occurring in the market to become less costly. Quality problems are not linear; they are diverse. Furthermore, quality characteristics are complicated because they differ for each product. The objective is to minimize losses to the extent possible by identifying the cause or causes of the problem. Quality engineers attempt to provide stable and high-quality products by improving product quality. However, two problems of production quality (shipping-side standard) and customer quality (accepting-side standard) must be solved. This problem is analyzed in detail in this paper. As a lead-time reduction example, we show that the lead time could be reduced by 20% by implementing a reorganization of the work process. We conduct production Test runs 1-3 in a production flow process, where Test runs 2 and 3 demonstrate almost the same excellent risk avoidance compared with Test run 1. These results are explained by Test runs 2 and 3 having less volatility in workers than Test run 1.

2. **Product Quality Probability Distribution (Normal Distribution) and Loss Function.** A manufacturing process that is termed as a production flow process is shown in Figure 1. The production flow process, which manufactures low volumes of a wide variety of products, is produced through several stages in the production process. In Figure 1, the process consists of six stages. In each step S1-S6 of the manufacturing process, material is being produced.

Figure 1 represents a manufacturing process called a flow production system, which is a manufacturing method employed in the production of control equipment. The flow production system, which in this case has six stages, is commercialized by the production of material in steps S1-S6 of the manufacturing process.

The direction of the arrow represents the direction of the production flow. With this system, production materials are supplied from the inlet and the end product will be shipped from the outlet.

Assumption 2.1. *The production structure is nonlinear.*

Assumption 2.2. *The production structure is a closed structure, that is, the production is driven by a cyclic system (production flow system).*

Assumption 2.1 indicates that the determination of the production structure is considered a major factor, which includes the generation value of production or the throughput generation structure in a stochastic manufacturing process (hereafter called the manufacturing field). Because such a structure is at least depending on the demand, it is considered to have a nonlinear structure.

Because the value of such a product depends on the throughput, its production structure is nonlinear. Therefore, Assumption 2.1 reflects the realistic production structure and is somewhat valid. Assumption 2.2 is completed in each step and flows from the next step

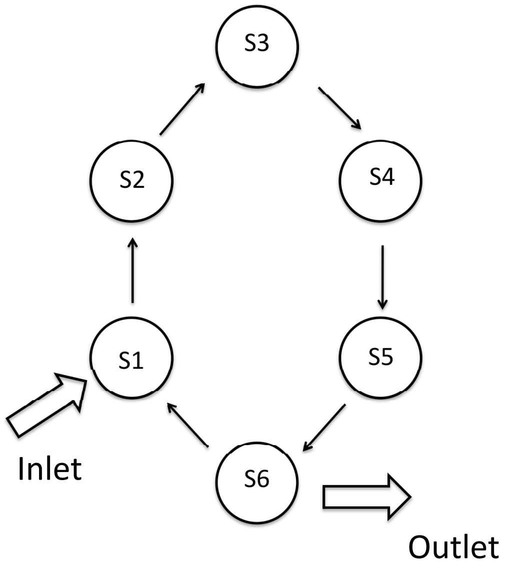

FIGURE 1. Production flow process

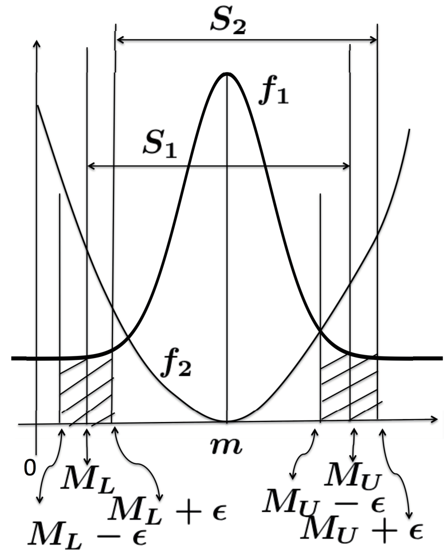

FIGURE 2. Production quality probability distribution $f(x)$ and loss function $L(x-m)$

until stage S6 is completed. Assumption 2.2 is reasonable because a new production starts from S1.

In Figure 2, f_1 represents the product quality, specifically the probability distribution function (normal distribution) of hybrid integrated chips. f_2 represents a loss function $L(x-m)$ for deviation from design value m. The loss function $L(x-m)$ is proportional to the volatility of the setting value. The loss function refers to quality troubles that occur in the market, and more details are listed below:

- No additive property value;
- Diversity of quality problems;
- Data for each individual product data for quality characteristics.

Parameters S_1 and S_2 represent the shipping-side standard and the accepting-side standard, respectively, and m represents the quality standard value. Parameters M_L (L: lower) and M_U (U: upper) represent the average value of nonstandard quality and the average value of excessive quality within the standard, respectively. Assume that ϵ is the same width for M_L and M_U. The shaded regions on the M_L side and on the M_U side in Figure 2 indicate the nonstandard quality and the excessive quality within the standard, respectively.

3. Boundary and Risk Analysis of the Hybrid Integrated IC Quality Distribution.

3.1. Boundary analysis of the hybrid integrated IC quality distribution. Figure 3 shows the normal distribution representing the product measurement value probability distribution near the tolerance boundary. The Jarque-Bera (JB) test is as follows [16]:

$$JB = \frac{n}{6}\left[S^2 + \frac{1}{4}(K-3)^3\right] \tag{1}$$

where n, S, and K are the sample size, the sample skewness, and the sample kurtosis, respectively.

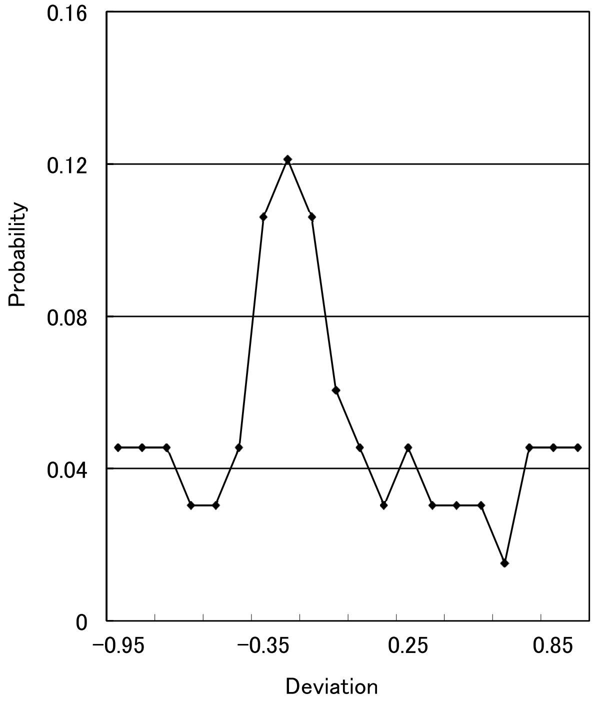

Figure 3. Normal distribution of the main manufacturing parts (hybrid IC)

Here good product width $16.0 < m < 22.0$, Average $= 20.95$, Volatility $= 0.332$, $N = 20$, $S \approx 1.617$, $K \approx 1.865$, and $JB \approx 9.793$. Therefore, Figure 3 was accepted as a normal distribution.

Regarding the theoretical value, the design value m as a good product is 17 to 18. $m = 16$ is the lower limit value of good products, and $m = 22$ is the upper limit value. Further, $m = 20.95$ is the best product average value of actual data.

Definition 3.1. *$f(x)$ denotes a probability density function of measured values for individual products.*

$$f(x) = \frac{dF(x)}{dx} = \frac{1}{\sqrt{2\pi}\sigma} \exp\left\{-\frac{(x-m)^2}{2\sigma^2}\right\} \tag{2}$$

where $F(x)$ denotes a probability distribution.

Definition 3.2. *$L(m - x)$ denotes a loss function for deviation from design value m.*

Here, The expected loss function $E[G(x)]$ is derived as follows:

$$E[G(x)] = \int_{M_L-\epsilon}^{M_L+\epsilon} f(x)L(x-m)dx + \int_{M_U-\epsilon}^{M_U+\epsilon} f(x)L(x-m)dx \tag{3}$$

Equation (3) denotes the expectation value of the loss due to the probability of the product function.

The quality problems occurring in the market have the following characteristics:

- No addition of the characteristic values;
- Diversity of quality problems;
- Non-reuse of data, that is, the quality characteristics depend on the data for each individual product.

We obtain the first term of right hand (*Lower*) in Equation (3) as follows:

$$Lower = F1 + F2 + F3 + S + T \tag{4}$$

where $F1$, $F2$, $F3$, S and T are as follows:

$$F1 = K\sigma^2\{\Phi(C_2) - \Phi(C_1)\}\left\{(C_2 - C_1)^2 - 2(C_2 - C_1) - \frac{1}{2}\right\} \quad (5)$$

$$F2 = 2Km\sigma\left[(C_2 - C_1)\{\Phi(C_2) - \Phi(C_1)\} - \frac{1}{2}\{\Phi(C_2) - \Phi(C_1)\}\right] \quad (6)$$

$$F3 = Km^2\{\Phi(C_2) - \Phi(C_1)\} \quad (7)$$

$$S = 2Km\sigma\left[(C_2 - C_1)\{\Phi(C_2) - \Phi(C_1)\}\right] - \frac{1}{2}\{\Phi(C_2) - \Phi(C_1)\} \quad (8)$$

$$T = Km^2\{\Phi(C_2) - \Phi(C_1)\} \quad (9)$$

We obtain the second term of right hand ($Upper$) in Equation (3) as follows:

$$Upper = B1 + B2 + B3 \quad (10)$$

where $B1$, $B2$ and $B3$ are as follows:

$$B1 = K\sigma^2\{\Phi(C_4) - \Phi(C_3)\}\left[(C_4 - C_3)^2 - 2(C_4 - C_3) - \frac{1}{2}\right] \quad (11)$$

$$B2 = 2Km\sigma\{(C_4 - C_3)\{\Phi(C_4) - \Phi(C_3)\}\} \quad (12)$$

$$B3 = Km^2\{\Phi(C_4) - \Phi(C_3)\} \quad (13)$$

With respect to the detailed calculation, refer Appendix A.

3.2. **Risk analysis of the hybrid integrated IC quality distribution.**

Definition 3.3. *Lead-time deviation* ΔT

$$\Delta T = (1 - P(T)) \times T \quad (14)$$

where $1 - P(T)$ *and* $P(T) = \Phi\left(\frac{m-\mu}{\sigma}\right)$ *denote the risk rate and normal probability respectively.*

Therefore, the lead-time including risk T_s' is defined as follows (Refer Appendix B).

Definition 3.4. *Lead-time including risk* T_s'

$$T_s' = T + \Delta T \quad (15)$$

The calculation results of Test runs 1-3 are represented in Table 1.

TABLE 1. Calculation results of Test runs 1-3

	T	ΔT	T_s'	Risk rate for workers
Test run 1	627	56	683	0.09
Test runs 2 and 3	400	4	404	0.01

With respect to Table 1, the process risk rates of Test run 1 and Test runs 2 and 3 were 0.1 and 0.05 respectively.

We describe the risk probability of Test runs 1-3. The probability distribution of the specific main part is a normal distribution. The normal distribution probability $P(T)$ in Equation (14) of the y-axis is shown when the x-axis (average value) is varied. The average and volatility in Table 2 are calculated on the basis of the data obtained from Test runs 1-3 (Appendix B). The case of Test run 1 is described. First, K1 to K9 are divided into three groups: A (K1, K4, K8), B (K2, K6, K9), and C (K3, K5, K7). The standard deviation of each working standard (WS) data is calculated, as are K1 to K9,

Table 2. Calculation results of Test runs 1-3

	Average of trend	Volatility	Final arrival value
Test run 1	0.83	0.175	0.9149
Test run 2	0.97	0.03	0.9996
Test run 3	0.95	0.04	0.9987

Table 3. Expected loss function including opportunity loss

	Volatility	Average	Cost rate	Upper value	Lower value	Low cost
Figure 4	0.33	1	1	1.5	0.6	2
Figure 5	0.1	1	1	1.5	0.6	4
Figure 6	0.1	0.7	1	0.6	0.2	1
Figure 7	0.1	0.5	1	1.5	1	3

Table 4. Expected loss function including opportunity loss

	Volatility	Ave.	C.rate	U.value	L.value	L.cost(U)	L.cost(L)
Figure 8	0.33	1	1	1.5	0.6	3	4
Figure 9	0.1	1	1	1.5	0.6	2	2
Figure 10	0.1	0.7	1	0.6	0.2	4	3
Figure 11	0.1	0.5	1	1.5	1	1	1

in Table 1; the average of K1 to K9 is then calculated. The volatility is the average value divided by 10. Refer to Appendix B for K1-K9, WS, and Test runs 1-3. The average value is obtained by averaging the work time of each group and normalizing the results. The final obtained value is the final probability value. The data for Test runs 2 and 3 in Table 2 are calculated via the same calculation as the test runs. As a result, Test runs 2 and 3 give almost the same excellent risk avoidance compared with Test run 1. This similarity is attributed to Test runs 2 and 3 having less volatility among workers than Test run 1.

With respect to Table 4, Ave., C.rate, U.value, L.value, L.cost(U) and L.cost(L) represent Average, Cost rate, Upper value, Lower value, Low cost(U) and Low cost(L).

4. **Verification of the Boundary and Risk Analysis of the Hybrid Integrated IC.**

4.1. **Numerical simulation of the boundary analysis.** Equation (40) represents the expected loss due to underquality that did not meet customer quality standards when the product was shipped. Similarly, Equation (47) conforms to the customer's quality standard when the product is shipped but represents the expected loss due to excessive quality.

Equation (33) represents products that are shipped but did not meet the customer's quality standards; that is, it represents the expected loss due to underquality. Similarly, Equation (47) represents products that conform to customer quality standards but are expected losses due to excessive quality.

Figures 4, 5, 6 and 7 cited in Table 3 and Figures 8, 9, 10 and 11 cited in Table 4 represent the expected loss function for nonstandard defective products and the expected loss function for excessive quality within standard, respectively. Figures 12, 13 and 14 cited in Table 5 and Figures 15, 16 and 17 cited in Table 6 show the ratio of occurrence of nonstandard defective products and nondefective products in comparison with design

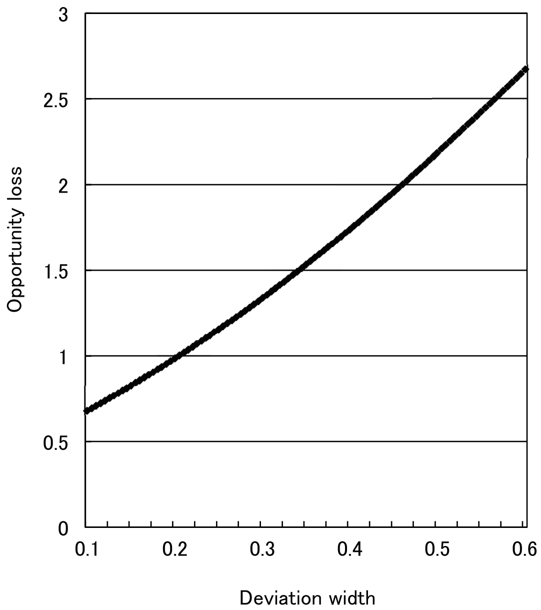

FIGURE 4. Expected loss function including opportunity loss

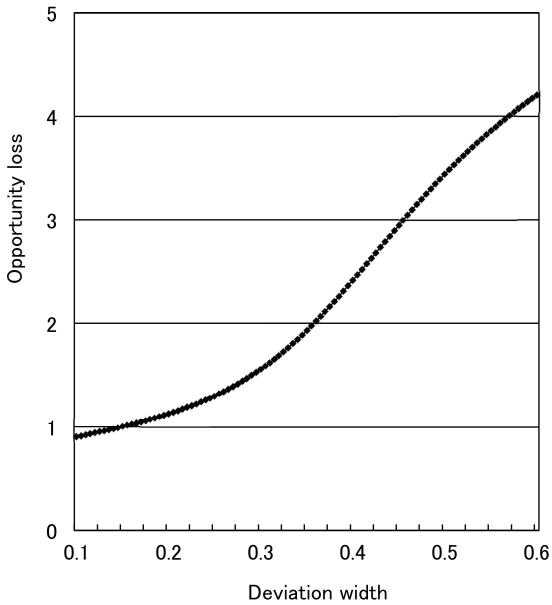

FIGURE 5. Expected loss function including opportunity loss

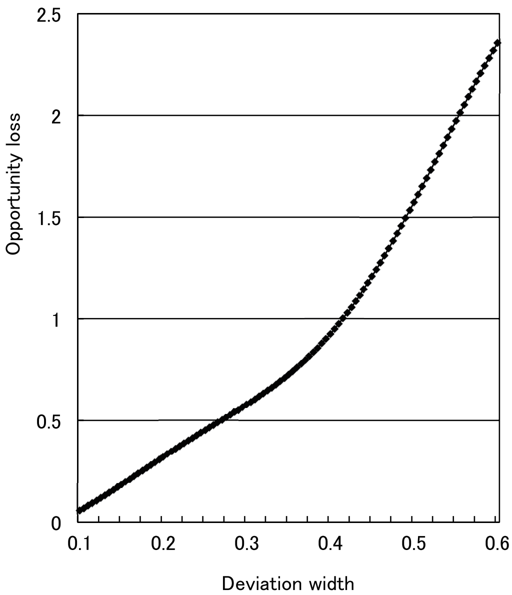

FIGURE 6. Expected loss function including opportunity loss

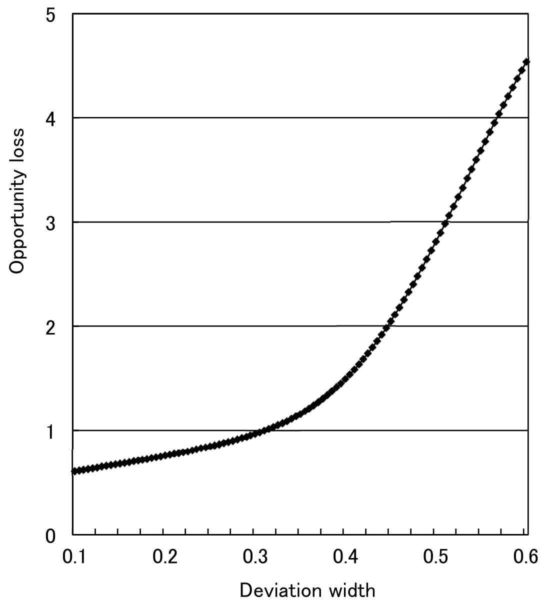

FIGURE 7. Expected loss function including opportunity loss

value, manufacturing variation, and cost rate respectively. The purpose of the figures in the cited figures is to enable cost reduction through optimization of the aforementioned parameters. The thick lines (Upper limit) and thin lines (Lower limit) in Figures 8 through 11 show the opportunity losses of nonstandard defective quality and excessive quality, respectively. The combination of parameters with a large loss order in both the upper and the lower values in Table 4 is

Figure 11 $>$ Figure 9 $>$ Figure 8 $>$ Figure 10.

However, when the upper/lower opportunity losses are summed, they are arranged in the order of the largest losses as

Figure 6 $>$ Figure 4 $>$ Figure 7 $>$ Figure 5.

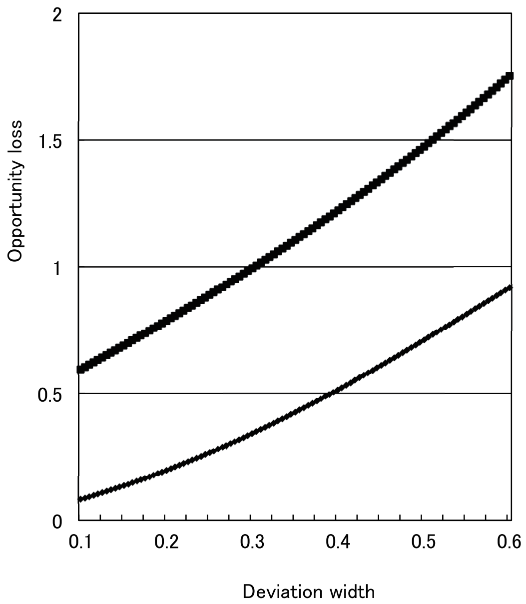

FIGURE 8. Expected loss function including opportunity loss -Comparison between upper limit and lower limit-

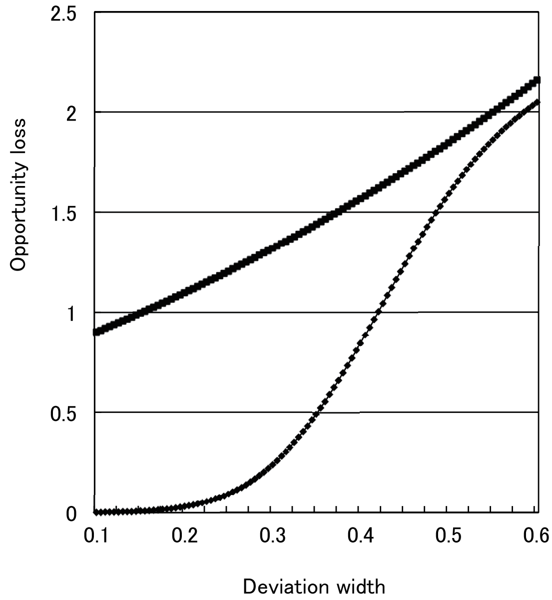

FIGURE 9. Expected loss function including opportunity loss -Comparison between upper limit and lower limit-

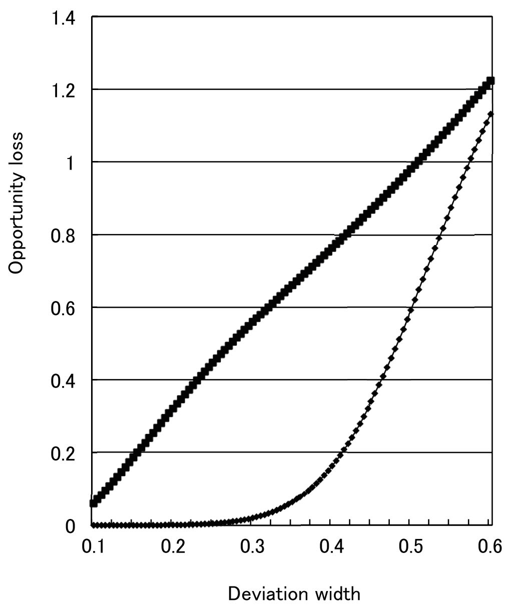

FIGURE 10. Expected loss function including opportunity loss -Comparison between upper limit and lower limit-

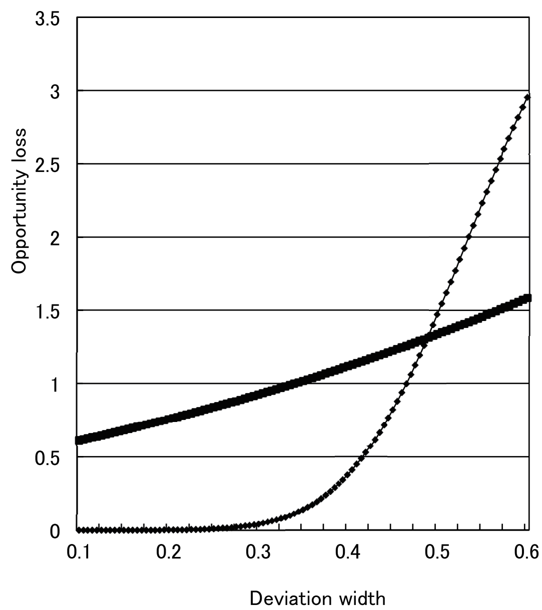

FIGURE 11. Expected loss function including opportunity loss -Comparison between upper limit and lower limit-

As a specific example, we consider the probability distribution of measurement data of major semiconductor parts used in certain products. This part is a custom-made hybrid integrated chip whose product quality is important. Figures 12, 13, and 14 are examples for M samples randomly selected among N $(N > M)$ lots. Therefore, the low cost order is

Figure 14 $>$ Figure 13 $>$ Figure 12.

TABLE 5. Expected loss function for nonstandard quality

	Design value	Volatility	Cost rate
Figure 12	1	0.6	7
Figure 13	1	0.45	7
Figure 14	1	0.33	7

TABLE 6. Expected loss function for excessive quality within standard

	Design value	Volatility	Cost rate
Figure 15	0.6	0.6	7
Figure 16	1	0.33	7
Figure 17	1	0.33	7

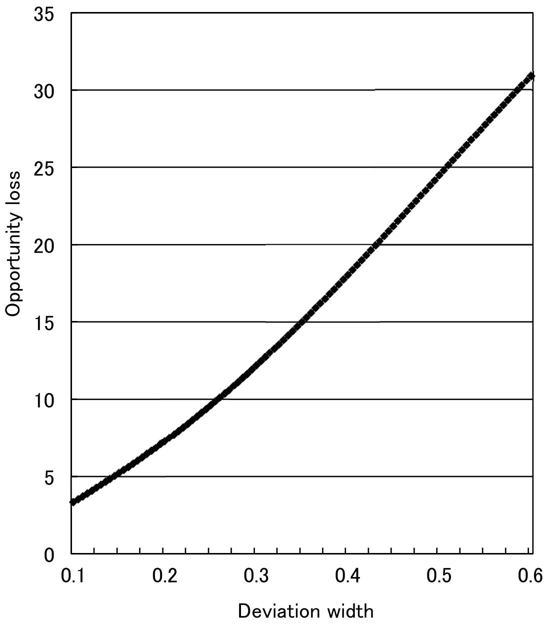

FIGURE 12. Expected loss function for nonstandard quality

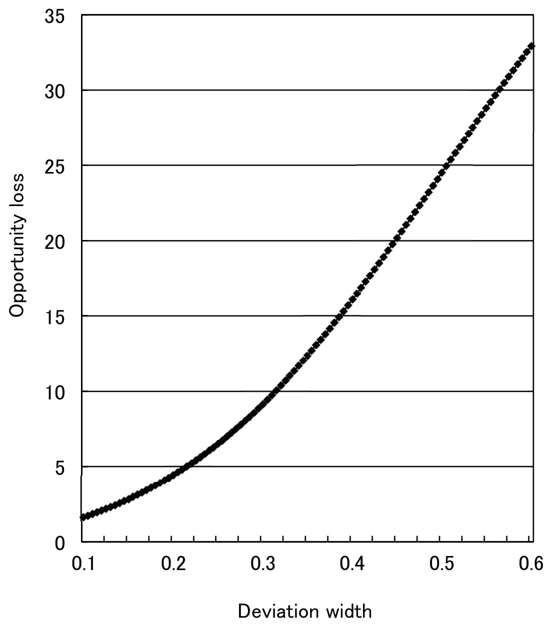

FIGURE 13. Expected loss function for nonstandard quality

Figures 15, 16, and 17 are also examples for M samples randomly selected among N ($N > M$) lots. Therefore, the low cost order is

Figure 17 > Figure 16 > Figure 15. Here, K and m denote the cost-rate and average respectively.

4.2. **Actual data analysis of the production lead time.** We present the actual data examples both the open and the cyclic production flow process having a nonlinearity. After we observed the nonlinear characteristics in the production process, we focused on an attempt to improve throughput [18]. At present, we have maintained a synchronized process. Using asynchronous logistics phenomenon and supply chain delays, we present a throughput improvement example, in which a production flow process is used for throughput improvement.

Here we investigate improved and standard process flows using a control device as an example. As a result, we found that according to throughput improvement post-process priority is appropriate. Using a buffer of the previous process to overcome bottlenecks

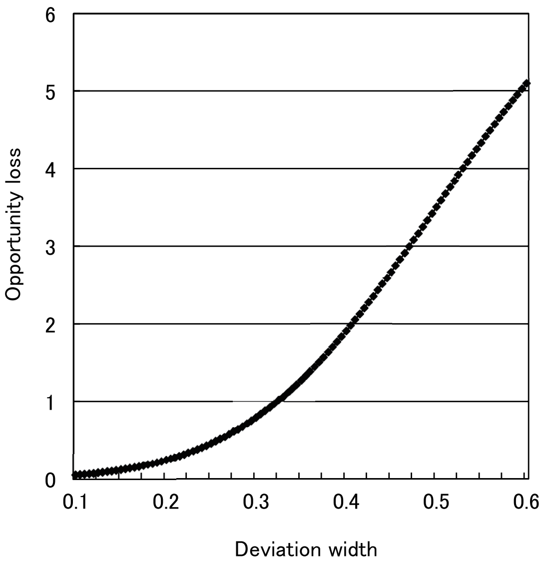

FIGURE 14. Expected loss function for nonstandard quality

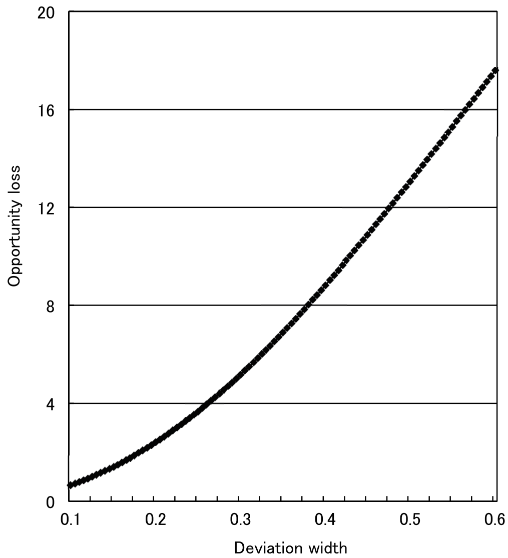

FIGURE 15. Expected loss function for excessive quality within standard

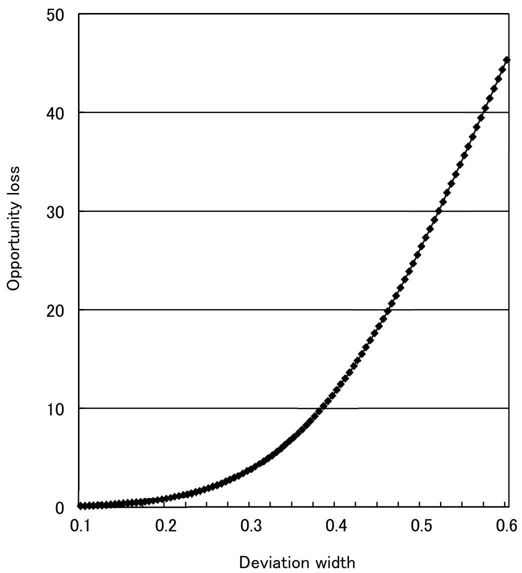

FIGURE 16. Expected loss function for excessive quality within standard

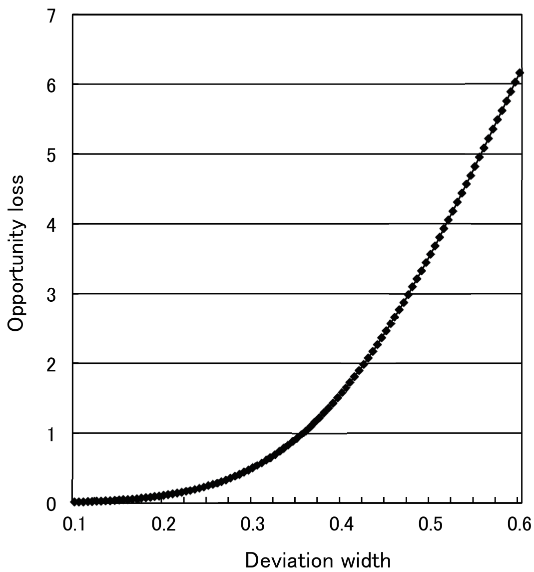

FIGURE 17. Expected loss function for excessive quality within standard

in the post process, the previous process can synchronize the post process, leading to significantly improved lead time.

Figure 18 illustrates the concept of process synchronization. Here X_{PR} represents the previous process, X_P represents the pre-work start date of the post process, and X_M represents the start date of the post process [18].

If we set the required production number $S(X_M)$ (i.e., required production number in a post process) to a synchronization point in time X_M, there is at least the following relationship between production numbers $S_P(X_{MP})$ among $[T_{MP}]$ and production numbers $S_R(X_{PR})$ among $[T_{MR}]$:

$$S_M(X_M) \leq S_P(X_{MP}) + S_R(X_{PR}) \tag{16}$$

where each symbol is as follows.

$$S_P(X_M) \equiv k_P \cdot [T_{MP}] \cdot n_P \tag{17}$$

$$S_R(X_{PR}) \equiv k_R \cdot [T_{MR}] \cdot n_R \tag{18}$$

Here n_P, n_R are the numbers of working people, k_P, k_R represent the process throughput variables (i.e., number of productions/all working people), and $[T_{MP}]$ and $[T_{MR}]$ represent the lead times of each period.

$$[T_{MP}] \equiv P_P[X_{MP}] > \bar{X}_P \cdot |X_M - X_P| \tag{19}$$

$$[T_{MR}] \equiv P_R[X_{PR}] > \bar{X}_R \cdot |X_M - X_{PR}| \tag{20}$$

where when $\bar{X}_P > 0$, $\bar{X}_P$ is integer and when $\bar{X}_R > 0$, $\bar{X}_R$ is integer.

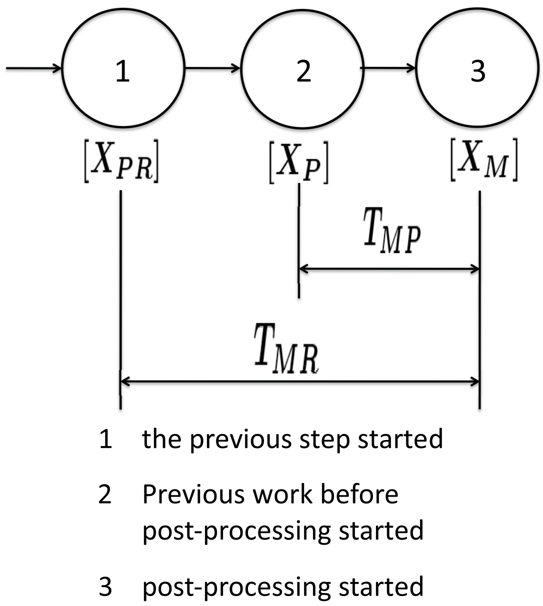

FIGURE 18. Conceptual diagram of the production process synchronization

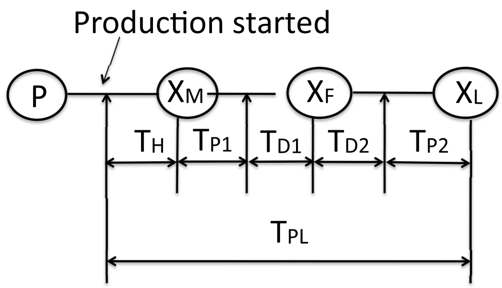

FIGURE 19. Production lead time in entire process

$P_P[X_{MP} > \bar{X}_P]$ and $P_R[X_{PR} > \bar{X}_R]$ are as follows:

$$P_P\left[X_{MP} > \bar{X}_P\right] = \Phi_P\left[\bar{X}_P/\sigma_{MP}\right] \tag{21}$$

$$P_R\left[X_{PR} > \bar{X}_R\right] = \Phi_R\left[\bar{X}_R/\sigma_{PR}\right] \tag{22}$$

where $\Phi_P[\bullet]$ and $\Phi_R[\bullet]$ represent standard normal distribution functions respectively.

Thus, the following can be established.

$$S_M \leq S_R + S_P \tag{23}$$

where $S_R > S_P$.

Equation (30) provides the relationship model of lead time and actual production manpower (input personnel). The lead time model is constructed from the model shown in Figure 19. We obtain several concepts from this model, i.e., the relationship between lead time and start date, the relationship between lead time and production manpower, and the lead time reduction equation. The model enables the consideration of the production flow.

Ideally, the relationship between production lead times and production start date in real companies is defined quantitatively. In particular, we select typical production equipment with different specifications for production and measure the final inspection time from start time to production completion. For any unforeseen situation, using statistical data, we can determine specific numerical targets.

We focus on the lead times of off-premise and on-premise production. In Figure 19, T_{PL} represents the production lead time, T_{P1} represents the production lead time for off-premise production (stochastic variable including deviation), T_{P2} represents the production lead time for on-premise production (stochastic variable including deviation), T_{D1} represents the residence time (idle time) of on-premise production, and T_H represents a previous process (harness processing). Thus, the production lead time can be obtained as follows.

$$T_{PL} = (T_{P1} + T_{P2}) + (T_{D1} + T_{D2}) + T_H \tag{24}$$

Here the production lead time is obtained from X_P (starting date) until X_L (production completion date) and is described as follows.

$$T_{PL} = |X_L - X_P| \tag{25}$$

If $P[T_{LM} > T_{PL}]$ provides a deviation of $|X_L - X_M|$, the evaluation of T_{DP}, which provides the production lead time of an actual process, is described as follows.

$$T_{DP} \leq T_{LM} - (T_{D1} + T_{D2}) \tag{26}$$

$$T_{DP} = P[T_{LM} > T_{PL}] \cdot |X_L - X_M| - (T_{D1} + T_{D2}) \tag{27}$$

where $T_{LM} = |X_L - X_M|$.

Here we refer to $P[T_{LM} > T_{PL}]$ as an incompatibility factor versus $|X_L - X_M|$, where M is any positive integer.

4.3. **Actual data example of lead time reduction by process recombination.** If the risk rate is 5%, $|X_L - X_M| = 18$ (date) and $(T_{D1} + T_{D2}) = 5$ (days); thereafter, T_{DP} can be obtained as follows.

$$T_{DP} \leq 0.95 \times 18 - 5 = 12 \tag{28}$$

From Equation (28), a post process must be completed within 12 days.

From the above description, we can evaluate the standard lead time in a post process in advance. Therefore, if the standard lead time is measured as $[T_{LM}]_{nom.}(h)$, the production lead time is as follows.

$$[T_{PL}]_{nom.} \geq \frac{[T_{LM}]_{nom.}(h) + T_H(h)}{8n(people)} \tag{29}$$

Thus, we can conduct a production process within the standard process time. We rewrite Equation (29) for $n(people)$. Then, we can obtain the production lead time as follows.

$$n \geq \frac{[T_{LM}]_{nom.}(h) + T_H(h)}{8 \cdot [T_{PL}]_{nom.}} \tag{30}$$

Figure 20 can be obtained from Equation (29). Figure 21 illustrates the standard production flow for equipment and represents a real production flow diagram rather than the lead time concept shown in Figure 19. Figure 23 illustrates the measurement lead time for a real production number. From the above description, if n_P and n_R are fixed, we have no choice but to alter the production rate to satisfy the synchronization condition. Considering risk in lead times, it is best to employ process flattening and process coupling.

To control the production capacity variable, we must deploy fair and flexible manpower planning and measure the lead time of production equipment. Figure 21 shows a standard production flow, and Figure 22 illustrates an improved flow obtained by flattening a cable production process. By incorporating a cable production process as a pre-process, we

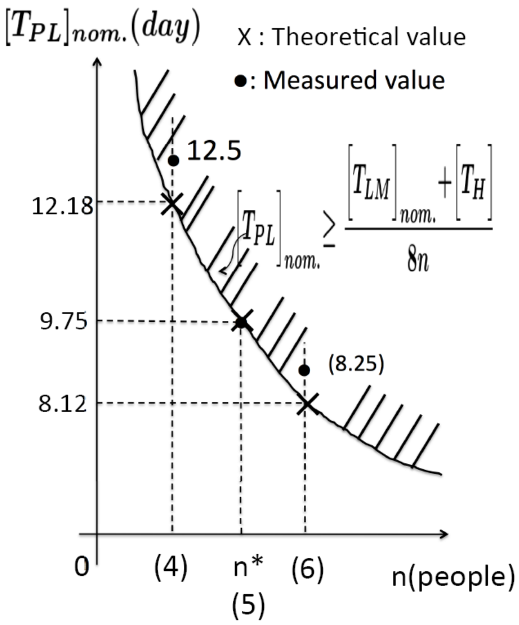

Figure 20. Relationship between lead time and work people

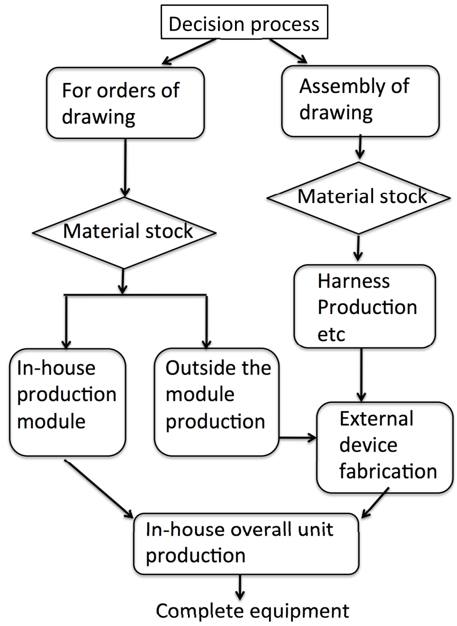

Figure 21. Standard equipment fabrication flow 1

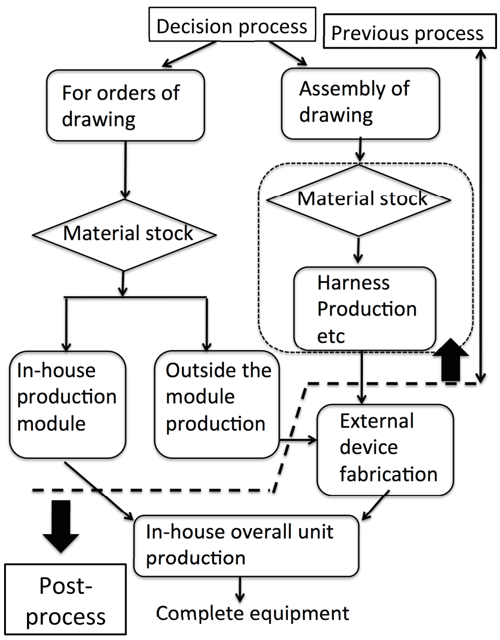

Figure 22. Improved equipment fabrication flow 2

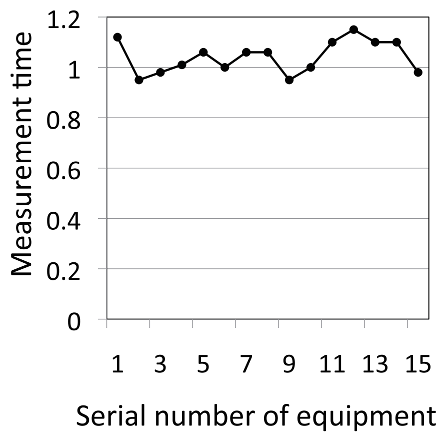

Figure 23. Production lead time variability

were able to obtain an improved process. Figure 23 shows the measurement results of production lead time from data obtained for a produced device. Here after receiving an order to manufacture equipment and confirming parts distribution, we can determine the start date by considering the delivery date, as is shown in Figure 23.

Then, Figure 23 provides the actual measurement data, which is the lead time of each process and time until final inspection is completed from the start date of production.

The production lead times are obtained by (measurement lead time)/(standard lead time).

Here the average production lead time is 1.0275 and the standard deviation is 0.051. From these results, the production lead times are relatively stable; however, a minor difference occurs in production lead times due to production equipment specifications.

Thus, we calculate the reduction rate of lead time to obtain (improved production flow)/(standard production flow) = 0.826 in the improved production flow 1, and (improved production flow)/(standard production flow) = 0.7239 in the improved production flow 2.

Therefore, the reduction rate of lead time is improved by approximately 13% in the improved production flow 1 and is improved by approximately 20% in the improved production flow 2. Here we define a throughput coefficient based on a standard production flow as follows.

Definition 4.1. *Throughput coefficient based on a standard production flow*

$$\eta \equiv \frac{[\textit{Number of production man-power}] \times [\textit{Number of real working time}]}{[\textit{Production risk rate}] \times [\textit{Reduction rate of lead time}]} \times \frac{1}{[\textit{Real working time of lead time}]} \tag{31}$$

If the numerator is constant, i.e., [production risk rate] = 1 and [real lead time] = constant, $\eta \cong 1.21$ (21% increase) in the improved production flow 1 and $\eta \cong 1.35$ (35% increase) in the improved production flow 2.

From the above description, by using a previous process as a buffer in a post process, we can realize synchronization between a previous process and post process. In other words, we have realized a post process with priority higher than the previous process.

5. Conclusions.

By introducing the product quality probability distribution (normal distribution) $f(x)$ and the loss function $L(x-m)$, we calculated the probability of occurrence of nonstandard defective products and excessive quality of nonstandard products within the standard, respectively. This approach enabled a quantitative assessment of the quality cost. In future work, we will report on cases where the product quality probability distribution is a lognormal distribution.

REFERENCES

[1] H. Yano, Learn about QE, *Robust Quality Engineering Society*, vol.20, no.2, pp.228-242, 1956.

[2] S. J. Baderstone and V. J. Mabin, A review Goldratt's theory of constraints (TOC) – Lessons from the international literature, *Operational Research Society of New Zealand the 33rd Annual Conference*, University of Auckland, New Zealand, 1998.

[3] K. Shirai, Y. Amano and S. Omatu, Improving throughput by considering the production process, *International Journal of Innovative Computing, Information and Control*, vol.9, no.12, pp.4917-4930, 2013.

[4] K. Shirai and Y. Amano, Analysis of fluctuations in production processes using Burgers equation, *International Journal of Innovative Computing, Information and Control*, vol.12, no.5, pp.1615-1628, 2016.

[5] K. Shirai and Y. Amano, Synchronization analysis of the production process utilizing the phase-field model, *International Journal of Innovative Computing, Information and Control*, vol.12, no.5, pp.1597-1613, 2016.

[6] K. Shirai and Y. Amano, Production density diffusion equation propagation and production, *IEEJ Trans. Electronics, Information and Systems*, vol.132-C, no.6, pp.983-990, 2012.

[7] K. Shirai and Y. Amano, Investigation of the relation between production density and lead-time via stochastic analysis, *International Journal of Innovative Computing, Information and Control*, vol.13, no.4, pp.1117-1133, 2017.

[8] H. Tasaki, *Thermodynamics – A Contemporary Perspective (New Physics Series)*, Baifukan, Co., LTD, 2000.
[9] K. Shirai and Y. Amano, Nonlinear characteristics of the rate of return in the production process, *International Journal of Innovative Computing, Information and Control*, vol.10, no.2, pp.601-616, 2014.
[10] K. Shirai, Y. Amano and S. Omatu, Propagation of working-time delay in production, *International Journal of Innovative Computing, Information and Control*, vol.10, no.1, pp.169-182, 2014.
[11] P. Wilmott, *Derivatives*, John Wiley & Sons, 1998.
[12] X. Wang and L. Xu, Study on the long-term rate of return when holding risk asset, *International Journal of Innovative Computing, Information and Control*, vol.6, no.7, pp.3275-3288, 2010.
[13] X. Wang, L. Xu and Q. Fang, The critical curve of the long-term rate of return when holding risk assets, *International Journal of Innovative Computing, Information and Control*, vol.6, no.10, pp.4579-4592, 2010.
[14] K. Shirai and Y. Amano, Analysis of production processes using a lead-time function, *International Journal of Innovative Computing, Information and Control*, vol.12, no.1, pp.125-138, 2016.
[15] K. Shirai and Y. Amano, Determination of allocation rate of production projects utilizing risk-sensitive control theory, *International Journal of Innovative Computing, Information and Control*, vol.13, no.3, pp.847-871, 2017.
[16] K. Shirai and Y. Amano, Self-similarity of fluctuations for throughput deviations within a production process, *International Journal of Innovative Computing, Information and Control*, vol.10, no.3, pp.1001-1016, 2014.
[17] K. Shirai, Y. Amano and S. Omatu, Process throughput analysis for manufacturing process under incomplete information based on physical approach, *International Journal of Innovative Computing, Information and Control*, vol.9, no.11, pp.4431-4445, 2013.
[18] K. Shirai and Y. Amano, A study on mathematical analysis of manufacturing lead time – Application for deadline scheduling in manufacturing system, *IEEJ Trans. Electronics, Information and Systems*, vol.132-C, no.12, pp.1973-1981, 2012.

Appendix A. Calculation of Equation (32).

$$E[G(x)] = \int_{M_L-\epsilon}^{M_L+\epsilon} f(x)L(x-m)dx + \int_{M_U-\epsilon}^{M_U+\epsilon} f(x)L(x-m)dx \tag{32}$$

The first term (A) of Equation (32) is derived as follows:

$$\int_{M_L-\epsilon}^{M_L+\epsilon} f(x)L(x-m)dx = \int_{M_L-\epsilon}^{M_L+\epsilon} \exp\left\{-\frac{(x-m)^2}{2\sigma^2}\right\}\left(Kx^2 - 2Kmx + Km^2\right)dx \tag{33}$$

$$\begin{aligned} &\text{First term of right hand in Equation (33)}\\ &= \frac{1}{\sqrt{2\pi}\sigma}\int_{M_L-\epsilon}^{M_L+\epsilon} \exp\left\{-\frac{(x-m)^2}{2\sigma^2}\right\}Kx^2dx \end{aligned} \tag{34}$$

$$\begin{aligned} &\text{Second term of right hand in Equation (33)}\\ &= -2Km\frac{1}{\sqrt{2\pi}\sigma}\int_{M_L-\epsilon}^{M_L+\epsilon} \exp\left\{-\frac{(x-m)^2}{2\sigma^2}\right\}Kx^2dx \end{aligned} \tag{35}$$

$$\begin{aligned} &\text{Third term of right hand in Equation (33)}\\ &= Km^2\frac{1}{\sqrt{2\pi}\sigma}\int_{M_L-\epsilon}^{M_L+\epsilon} \exp\left\{-\frac{(x-m)^2}{2\sigma^2}\right\}Kx^2dx \end{aligned} \tag{36}$$

We perform the following variable transformation.

$$\begin{aligned} z &= \frac{x-m}{\sigma} \Rightarrow dx = \sigma dz\\ C_1 &= \frac{D_1 - m}{\sigma} : D_1 = M_L - \epsilon \end{aligned} \tag{37}$$

$$C_2 = \frac{D_2 - m}{\sigma} : D_2 = M_L + \epsilon \tag{38}$$

$$dx = \sigma dz \tag{39}$$

Then, we obtain as follows:

$$\begin{aligned}
\text{Equation (34)} &= K\frac{1}{\sqrt{2\pi}}\int_{C_1}^{C_2} \exp\left\{-\frac{1}{2}z^2\right\}(\sigma z + m)^2 dz \\
&= K\frac{1}{\sqrt{2\pi}}\int_{C_1}^{C_2} \exp\left\{-\frac{1}{2}z^2\right\}\left(\sigma^2 z^2 + 2m\sigma z + m^2\right) dz \\
&= \frac{K}{\sqrt{2\pi}}\sigma^2\int_{C_1}^{C_2} z^2 \exp\left\{-\frac{1}{2}z^2\right\} dz + 2m\sigma\int_{C_1}^{C_2}\frac{K}{\sqrt{2\pi}} z\exp\left\{-\frac{1}{2}z^2\right\} dz \\
&\quad + m^2\int_{C_1}^{C_2}\frac{K}{\sqrt{2\pi}}\exp\left\{-\frac{1}{2}z^2\right\} dz
\end{aligned} \tag{40}$$

With respect to Equation (40), the first term $F1$ in right hand is calculated as follows:

$$\begin{aligned}
F1 &= \sigma^2\left[\left[z^2\right]_{C_1}^{C_2} \times \int_{C_1}^{C_2}\frac{K}{\sqrt{2\pi}}\exp\left\{-\frac{1}{2}z^2\right\} dz - 2\int_{C_1}^{C_2} z\frac{K}{\sqrt{2\pi}}\exp\left\{-\frac{1}{2}z^2\right\} dz\right] \\
&= \sigma^2\left[\left[z^2\right]_{C_1}^{C_2} \times \int_{C_1}^{C_2}\frac{K}{\sqrt{2\pi}}\exp\left\{-\frac{1}{2}z^2\right\} dz\right. \\
&\quad \left. -2\left\{[z]_{C_1}^{C_2} \times \int_{C_1}^{C_2}\frac{K}{\sqrt{2\pi}}\exp\left\{-\frac{1}{2}z^2\right\} dz\right\} - \frac{1}{2}\int_{C_1}^{C_2}\frac{K}{\sqrt{2\pi}}\exp\left\{-\frac{1}{2}z^2\right\} dz\right] \\
&= \sigma^2\left[\left[z^2\right]_{C_1}^{C_2} \times \left\{\int_{C_2}^{\infty}\frac{K}{\sqrt{2\pi}}\exp\left\{-\frac{1}{2}z^2\right\} dz - \int_{C_1}^{\infty}\frac{K}{\sqrt{2\pi}}\exp\left\{-\frac{1}{2}z^2\right\} dz\right\}\right. \\
&\quad - 2\left\{[z]_{C_1}^{C_2} \times \left\{\int_{C_2}^{\infty}\frac{K}{\sqrt{2\pi}}\exp\left\{-\frac{1}{2}z^2\right\} dz - \int_{C_1}^{\infty}\frac{K}{\sqrt{2\pi}}\exp\left\{-\frac{1}{2}z^2\right\} dz\right\}\right. \\
&\quad \left.\left. -\frac{1}{2}\left\{\int_{C_2}^{\infty}\frac{K}{\sqrt{2\pi}}\exp\left\{-\frac{1}{2}z^2\right\} dz - \int_{C_1}^{\infty}\frac{K}{\sqrt{2\pi}}\exp\left\{-\frac{1}{2}z^2\right\} dz\right\}\right\}\right] \\
&= K\sigma^2\left[\left[z^2\right]_{C_1}^{C_2} \times \{\Phi(C_2) - \Phi(C_1)\} - 2\left[z^2\right]_{C_1}^{C_2} \times \{\Phi(C_2) - \Phi(C_1)\}\right. \\
&\quad \left. -\frac{1}{2}\{\Phi(C_2) - \Phi(C_1)\}\right] \\
&= K\sigma^2\{\Phi(C_2) - \Phi(C_1)\}\left\{(C_2 - C_1)^2 - 2(C_2 - C_1) - \frac{1}{2}\right\}
\end{aligned} \tag{41}$$

Then, the second term of Equation (40) is calculated as follows:

$$F2 = 2Km\sigma\left[(C_2 - C_1)\{\Phi(C_2) - \Phi(C_1)\} - \frac{1}{2}\{\Phi(C_2) - \Phi(C_1)\}\right] \tag{42}$$

Finally, the third term of Equation (40) is calculated as follows:

$$F3 = Km^2\{\Phi(C_2) - \Phi(C_1)\} \tag{43}$$

The second term S in Equation (34) is calculated as follows:

$$S = 2m\sigma\left[[z]_{C_1}^{C_2} \times \int_{C_1}^{C_2}\frac{K}{\sqrt{2\pi}}\exp\left\{-\frac{1}{2}z^2\right\} dz\right] - \frac{1}{2}\int_{C_1}^{C_2}\frac{K}{\sqrt{2\pi}}\exp\left\{-\frac{1}{2}z^2\right\} dz$$

$$= 2Km\sigma \left[(C_2 - C_1) \left\{ \Phi(C_2) - \Phi(C_1) \right\} \right] - \frac{1}{2} \left\{ \Phi(C_2) - \Phi(C_1) \right\} \tag{44}$$

The third term T in Equation (34) is calculated as follows:

$$T = Km^2 \int_{C_1}^{C_2} \frac{K}{\sqrt{2\pi}} \exp\left\{ -\frac{1}{2} z^2 \right\} dz = Km^2 \left\{ \Phi(C_2) - \Phi(C_1) \right\} \tag{45}$$

Therefore, Equation (34) can be calculated as follows:

$$\text{Equation (34)} = F1 + F2 + F3 + S + T \tag{46}$$

With respect to the second term (B) of Equation (32), according to Equation (40), we obtain as follows:

$$\begin{aligned} B = {} & \sigma^2 \int_{C_3}^{C_4} \frac{K}{\sqrt{2\pi}} z^2 \exp\left\{ -\frac{1}{2} z^2 \right\} dz + 2m\sigma \int_{C_3}^{C_4} \frac{K}{\sqrt{2\pi}} z \exp\left\{ -\frac{1}{2} z^2 \right\} dz \\ & + m^2 \int_{C_3}^{C_4} \frac{K}{\sqrt{2\pi}} \exp\left\{ -\frac{1}{2} z^2 \right\} dz \end{aligned} \tag{47}$$

where z, C_3 and C_4 are derived as follows:

$$z = \frac{x - m}{\sigma} \Rightarrow dx = \sigma dz$$

$$C_3 = \frac{D_3 - m}{\sigma} : D_3 = M_U - \epsilon \tag{48}$$

$$C_4 = \frac{D_4 - m}{\sigma} : D_4 = M_U + \epsilon \tag{49}$$

$$dx = \sigma dz \tag{50}$$

The first term $B1$ of Equation (47) is calculated as follows:

$$B1 = K\sigma^2 \{\Phi(C_4) - \Phi(C_3)\} \left[(C_4 - C_3)^2 - 2(C_4 - C_3) - \frac{1}{2} \right] \tag{51}$$

According to the second term of Equation (42), we obtain the second term $B2$ of Equation (47) as follows:

$$B2 = 2Km\sigma \left\{ (C_4 - C_3) \left\{ \Phi(C_4) - \Phi(C_3) \right\} \right\} \tag{52}$$

According to the third term of Equation (42), we obtain the third term $B3$ of Equation (47) as follows:

$$B3 = Km^2 \{\Phi(C_4) - \Phi(C_3)\} \tag{53}$$

As a result, Equation (47) can be calculated by Equations (51), (52) and (53).

Consequently, the expected opportunity loss function $E(G(x)]$ is calculated by Equations (40) and (53). Therefore, Equation (47) can be calculated as follows:

$$\text{Equation (47)} = B1 + B2 + B3 \tag{54}$$

Appendix B. **Analysis of Actual Data Test Run Results in the Production Flow System.**

- (Test run 1) Because the throughput of each process (S1-S6) is asynchronous, the overall process throughput is asynchronous. In Table 8, we list the manufacturing time (min) of each process. In Table 9, we list the volatility in each process performed by the workers. Finally, Table 8 lists the target times. The theoretical throughput is obtained as $3 \times 199 + 2 \times 15 = 627$ (min). In addition, the total working time in stage S3 is 199 (min), which causes a bottleneck. In Figure 24, we plot the measurement data listed in Table 8, which represents the total working time of each worker (K1-K9). In Figure 25, we plot the data contained in Table 8, which represents the volatility of the working times.

- (Test run 2) Set to synchronously process the throughput. The target time listed in Table 10 is 500 (min), and the theoretical throughput (not including the synchronization idle time) is 400 (min). Table 11 presents the volatility of each working process (S1-S6) for each worker (K1-K9).
- (Test run 3) Introducing a preprocess stage. The process throughput is performed synchronously with the reclassification of the process. As shown in Table 12, the theoretical throughput (not including the synchronization idle time) is 400 (min). Table 13 presents the volatility of each working process (S1-S6) for each worker (K1-K9). On the basis of these results, the idle time must be set to 100 (min). Moreover, the theoretical target throughput (T_s') can be obtained using the "Synchronization with preprocess" method. This goal is as follows:

$$\begin{aligned} T_s &\sim 20 \times 6(\text{First cycle}) + 17 \times 6(\text{Second cycle}) \\ &\quad + 20 \times 6(\text{Third cycle}) + 20(\text{Previous process}) + 8(\text{Idol-time}) \\ &\sim 370 \text{ (min)} \end{aligned} \tag{55}$$

The full synchronous throughput in one stage (20 min) is

$$T_s' = 3 \times 120 + 40 = 400 \text{ (min)} \tag{56}$$

Using the "Synchronization with preprocess" method, the throughput is reduced by approximately 10%. Therefore, we showed that our proposed "Synchronization with preprocess" method is realistic and can be applied in flow production systems. Below, we represent for a description of the "Synchronization with preprocess".

In Table 12, the working times of the workers K4, K7 show shorter than others. However, the working time shows around target time. Next, we manufactured one piece of equipment in three cycles. To maintain a throughput of six units/day, the production throughput must be as follows:

$$\frac{(60 \times 8 - 28)}{3} \times \frac{1}{6} \simeq 25 \text{ (min)} \tag{57}$$

where the throughput of the preprocess is set to 20 (min). In Equation (57), the value 28 represents the throughput of the preprocess plus the idle time for synchronization. Similarly, the number of processes is 8 and the total number of processes is 9 (8 plus the preprocess). The value of 60 is obtained as 20 (min) × 3 (cycles).

In Table 7, Test run 3 indicates a best value for the throughput in the three types of theoretical working time. Test run 2 is ideal production method. However, because it is difficult for talented worker, Test run 3 is a realistic method. The working time does not include the idle time.

The results are as follows. Here, the trend coefficient, which is the actual number of pieces of equipment/the target number of equipment, represents a factor that indicates the degree of the number of pieces of manufacturing equipment.
Test run 1: 4.4 (pieces of equipment)/6 (pieces of equipment) = 0.73,
Test run 2: 5.5 (pieces of equipment)/6 (pieces of equipment) = 0.92,
Test run 3: 5.7 (pieces of equipment)/6 (pieces of equipment) = 0.95.
Volatility data represent the average value of each Test-run.

TABLE 7. Correspondence between the table labels and the test run number

	Table Number	Production process	Working time	Volatility
Test run 1	Table 8	Asynchronous process	627 (min)	0.29
Test run 2	Table 10	Synchronous process	400 (min)	0.06
Test run 3	Table 12	"Synchronization with preprocess" method	400 (min)	0.03

TABLE 8. Total manufacturing time at each stage for each worker

	WS	S1	S2	S3	S4	S5	S6
K1	15	20	20	25	20	20	20
K2	20	22	21	22	21	19	20
K3	10	20	26	25	22	22	26
K4	20	17	15	19	18	16	18
K5	15	15	20	18	16	15	15
K6	15	15	15	15	15	15	15
K7	15	20	20	30	20	21	20
K8	20	29	33	30	29	32	33
K9	15	14	14	15	14	14	14
Total	145	172	184	199	175	174	181

TABLE 9. Volatility of Table 8

K1	1.67	1.67	3.33	1.67	1.67	1.67
K2	2.33	2	2.33	2	1.33	1.67
K3	1.67	3.67	3.33	2.33	2.33	3.67
K4	0.67	0	1.33	1	0.33	1
K5	0	1.67	1	0.33	0	0
K6	0	0	0	0	0	0
K7	1.67	1.67	5	1.67	2	1.67
K8	4.67	6	5	4.67	5.67	6
K9	0.33	0.33	0	0.33	0.33	0.33

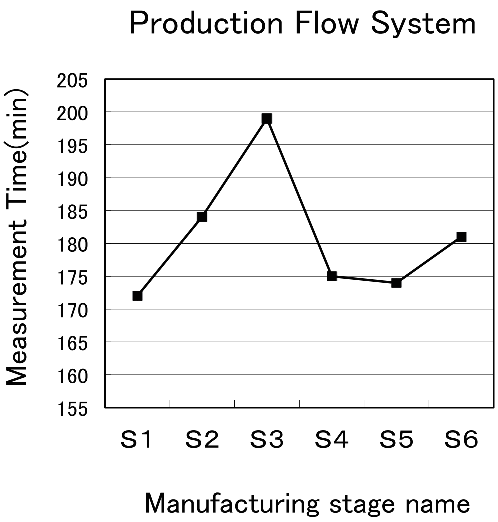

FIGURE 24. Total work time for each stage (S1-S6) in Table 8

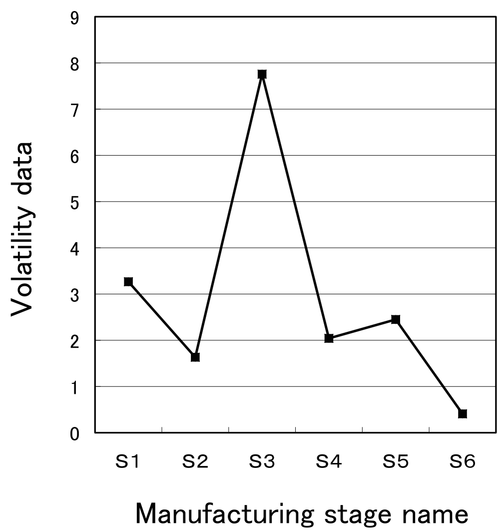

FIGURE 25. Volatility data for each stage (S1-S6) in Table 8

Table 10. Total manufacturing time at each stage for each worker

	WS	S1	S2	S3	S4	S5	S6
K1	20	20	24	20	20	20	20
K2	20	20	20	20	20	22	20
K3	20	20	20	20	20	20	20
K4	20	25	25	20	20	20	20
K5	20	20	20	20	20	20	20
K6	20	20	20	20	20	20	20
K7	20	20	20	20	20	20	20
K8	20	27	27	22	23	20	20
K9	20	20	20	20	20	20	20
Total	180	192	196	182	183	182	180

Table 11. Volatility of Table 10

K1	0	1.33	0	0	0	0
K2	0	0	0	0	0.67	0
K3	0	0	0	0	0	0
K4	1.67	1.67	0	0	0	0
K5	0	0	0	0	0	0
K6	0	0	0	0	0	0
K7	0	0	0	0	0	0
K8	2.33	2.33	0.67	1	0	0
K9	0	0	0	0	0	0

Table 12. Total manufacturing time at each stage for each worker, K5 (*): Preprocess

	WS	S1	S2	S3	S4	S5	S6
K1	20	18	19	18	18	18	18
K2	20	18	18	18	18	18	18
K3	20	21	21	21	21	21	21
K4	16	13	11	11	13	13	13
K5	16	*	*	*	*	*	*
K6	16	18	18	18	18	18	18
K7	16	14	14	13	14	14	13
K8	20	22	22	22	22	22	22
K9	20	20	20	20	20	20	20
Total	148	144	143	141	144	144	143

Table 13. Volatility of Table 12, K5 (*): Preprocess

K1	0.67	0.33	0.67	0.67	0.67	0.67
K2	0.67	0.67	0.67	0.67	0.67	0.67
K3	0.33	0.33	0.33	0.33	0.33	0.33
K4	1	1.67	1.67	1	1	1
K5	*	*	*	*	*	*
K6	0.67	0.67	0.67	0.67	0.67	0.67
K7	0.67	0.67	1	0.67	0.67	1
K8	0.67	0.67	0.67	0.67	0.67	0.67
K9	0	0	0	0	0	0